Cloud-Edge Collaboration Dynamics Information Dissemination Model for Social Internet of Things

Yuexia Zhang, *Member, IEEE*, Lie Zou, and Dawei Pan

***Abstract*—Studying the mechanism of information dissemination in Social Internet of Things (SIoT) has practical significance for real-time information control and scientific management decision-making in real world. Aiming at the problem of how to realize the information interaction between people, people and things, and things and things in SIoT, we propose a cloud-edge collaborative dynamic information dissemination model (CCDIDM) for SIoT. Firstly, considering the interactive influence of information dissemination between individual users, between IoT devices, and between users and devices, the coupling relationship between nodes is established. Based on the theory of dissemination dynamics, the information propagation process between coupled nodes of SIoT is analyzed, and the efficient interactive dissemination of information is simulated. Theoretical analysis of the model is carried out, and the information dissemination threshold and the stability of the equilibrium point are deduced. Simulation results are consistent with the theoretical analysis, demonstrating that CCDIDM can describe information dissemination. Simultaneously, it was found that, stronger the perception awareness of individual users, smaller the scale of information dissemination. In addition, the influence of various parameters on the scale of information dissemination is verified. Adjusting the size of such parameters can promote or inhibit the dissemination of information.**

***Index Terms*—Cloud-edge computing, information dissemination, information interaction, social Internet of Things.**

I. Introduction

THE advancement of internet technology in recent years has promoted the rapid development of Social Internet of Things (SIoT) [1], [2], [3], [4], [5], [6], which is a concept proposed through the combination of social networks [7], [8], [9] and Internet of Things (IoT) [10], [11], [12]. The attributes of social networks are introduced into the IoT to establish relationships between things–things, things–people, and people–people, so as to realize the connection, service, and application of the IoT. Examples of this include establishing a social network between vehicles to achieve information sharing between them [13], [14], [15] and establishing a social network between mobile phones, computers, smart home appliances, and other devices to realize information release between devices [16], [17]. The communication between things–things, things–people, and people–people in the SIoT generates a variety of information. Effective information interaction can improve the efficiency of information dissemination, enable people and things to obtain information in a timely manner, and further improve the quality of life. Eom et al. used the SIoT in the factory management system and proposed an autonomous demand-side management system architecture to solve the management problem of smart grid [18]. Marche et al. proposed an intelligent HVAC system based on the architecture of SIoT, which significantly reduced system energy consumption and realized the trade-off between energy cost and thermal comfort of users [19]. Therefore, the study of information dissemination on the SIoT is of great significance for comprehensively exploring the nature and laws of information dissemination and effectively controlling and predicting the dissemination of information.

At present, there are many reported studies on the information transmission of SIoT, and most scholars simulate and analyze the information transmission process of social networks and IoT, mainly based on the epidemic model [18], [19]. Wu et al. [20] established a social network SIR information dissemination model based on implicit links and social influence, by mining the implicit relationship between individual users and considering their influence, and analyzed the model's performance using mean field theory. The research results demonstrated that implicit links play an important role in driving user behavior, and the model can well explain the process of information dissemination. Ran et al. [21] further considered that the dissemination of information on social networks will be affected by the interference of external factors, and proposed the positive and negatively susceptible to exposed ignorant removal (PaNSEIR) model. Through analysis, it was concluded that external interference information greatly promotes the spread of information. Feng et al. [22] simulated the process of virus information dissemination on wireless sensor networks based on the SIRS model, theoretically analyzed the stability of information dissemination, and predicted

Manuscript received 18 October 2022; revised 22 December 2022; accepted 9 January 2023. Date of publication 12 January 2023; date of current version 16 June 2023. This work was supported in part by the Sub Project of National Key Research and Development plan in 2020 under Grant 2020YFC1511704, and in part by Beijing Science and Technology Project under Grant Z211100004421009. Recommended for acceptance by Chau Yuen. *(Corresponding author: Yuexia Zhang.)*

Yuexia Zhang is with the Key Laboratory of Information and Communication Systems, Ministry of Information Industry, Beijing Information Science and Technology University, Beijing 100101, China, and also with the Laboratory of the Ministry of Education for Optoelectronic Measurement Technology and Instrument, Beijing 100101, China (e-mail: zhangyuexia@bistu.edu.cn).

Lie Zou and Dawei Pan are with the School of Information and Communication Engineering, Beijing Information Science & Technology University, Beijing 100101, China (e-mail: zoulie1997@163.com; pandw9395@163.com).

Digital Object Identifier 10.1109/TNSE.2023.3236478

the dissemination scale of virus information. In addition, Ning et al. [23] proposed a social awareness-based information diffusion model for NB-IoT. By stimulating effective cooperation between user equipment, a multi-hop communication scheme for socially-aware terminals was introduced to improve the connectivity of links, thereby improving the efficiency of information dissemination. The above studies all focus on the dissemination process of information on a single-layer network, in which the dissemination mechanism is simple. However, real-world systems are not independent, and multiple networks interact.

To solve the problems regarding low accuracy of the single-layer propagation model and simple propagation mechanism, researchers have studied information propagation in multilayer networks. Yagan et al. [24] analyzed the information transmission between social networks and physical networks based on the SIR model, and deduced the scale and critical threshold of information transmission. Experiments showed that the combination of physical and social networks could affect the speed and scale of information transmission. Yao et al. [25] established the relationship between people and things in the SIoT based on the hypergraph, and improved the accuracy of information recommendation service in the SIoT by using the communication model of the social network. Qian et al. [26] analyzed the diffusion process of emergency information within social networks and the IoT, considering the contact strength and degree of interest between devices. They proposed a low-complexity emergency information diffusion strategy based on many-to-many matching, and demonstrated that this strategy can improve the speed and efficiency of emergency information dissemination. Information propagation in multilayer networks was analyzed in the above-mentioned studies. However, these studies failed to fully consider the impact of human-to-human social relationships on information dissemination between IoT devices, resulting in low information dissemination efficiency. Therefore, realizing the information interaction between people and people, people and things, and things and things in the SIoT, such that information can be effectively disseminated, is an urgent problem to be solved.

In order to solve the above problems, this paper proposes a cloud edge collaborative dynamics information dissemination model for SIoT to predict and control information dissemination in SIoT, so as to better realize the information interaction between people, people and things, and things and things in SIoT. The main contributions of this paper are as follows:

1) in SIoT network architecture, considering the interaction between individual users and interaction of information transmission between Internet equipment, and divide the user individual and state of smart device, the user individual node coupling with iot devices, coupling relationship of information transmission between nodes, to describe the process of information transmission in the IoT.
2) According to the characteristics of real-time processing and feedback of cloud edge, the relationship of communication mechanism is established, and a cloud edge collaborative dynamic information dissemination model for SIoT is proposed to achieve efficient information interaction and dissemination.

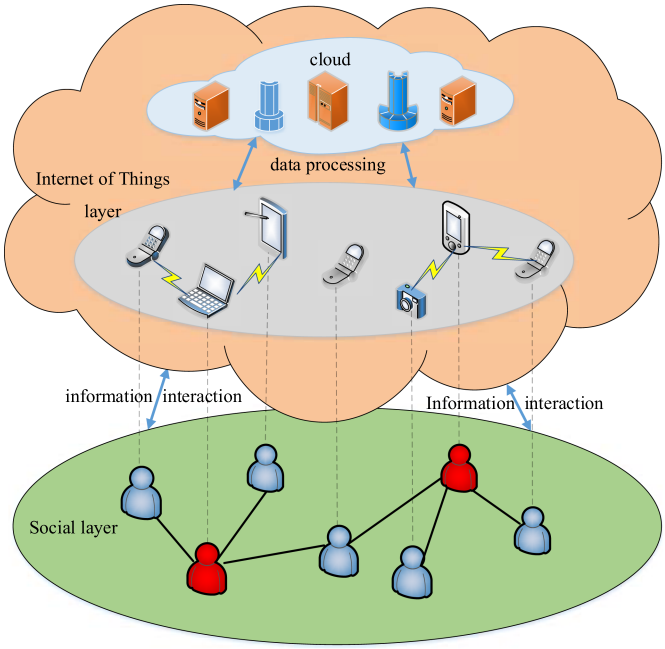

Fig. 1. Network architecture of Social Internet of Things.

3) The dynamic characteristics of the cloud edge cooperative dynamics information dissemination model are theoretically analyzed, including deriving the equilibrium point and information dissemination threshold, and the stability of the cloud edge cooperative dynamics information dissemination model at the equilibrium point is proved.
4) Verify the effectiveness of the information dissemination model of cloud edge collaborative dynamics through simulation experiments, analyze the influence of the dissemination mechanism on information dissemination, and conduct a detailed analysis of the experimental results.

II. System Model

In this section, the components of the SIoT are introduced in detail and are subsequently abstracted into a multilayer information dissemination model.

A. Social Internet of Things Description

The SIoT network architecture shown in Fig. 1 shows that SIoT consists of the social layer and the IoT layer.

The social layer is composed of different individual users, and there are corresponding interactions among them to enable the spread of information. The IoT layer consists of different smart devices (mobile phones, tablets, computers, etc.) and cloud servers. Smart devices have a certain computing power and can communicate information with each other. The cloud server is equipped with relatively powerful computing power, which can process the computing tasks of the smart devices held by individual users. When the smart device cannot handle the computing task, the task can be transferred to the cloud server through the wireless network. Since there is a one-to-one correspondence between individual users of social networks and smart devices

TABLE I
STATUS CLASSIFICATION OF INDIVIDUAL USERS IN THE SOCIAL LAYER OF SIOT

Individual user status	Status name	Status meaning
U	Unknown	The individual user is unaware of the information transmitted between smart devices, and may become exposed when they receive information from a neighboring individual or a matching device.
E	Exposed	The individual user knows the information transmitted between smart devices, is uncertain about the accuracy of the information, and is unwilling to spread the known behavior to their neighbors.
K	Known	The individual user knows the information transmitted between smart devices, can determine the accuracy of the information, and can propagate the known behavior to their neighbors.

In the social layer, the status of individual users is divided into three categories, according to the dissemination of information by the individual users: Unknown (U), Exposed (E) and Known (K). The specific meaning of each status of the individual user is given in TABLE I. The individual user follows the state transition rule of $U \to E \to K \to U$, $U \to E \to U$ and $U \to K \to U$ at the social layer.

of the IoT, when a smart device receives information from a neighboring smart device, the individual user will acquire the information. Simultaneously, depending on the behavior of individual users regarding information dissemination, this may lead to information dissemination and interactions between individual users, and frequent interactions between individual users will ultimately affect the dissemination of information on smart devices.

In the social layer, the status of individual users is divided into three categories, according to the dissemination of information by the individual users: Unknown (U), Exposed (E) and Known (K). The specific meaning of each status of the individual user is given in Table I. The individual user follows the state transition rule of $U \to E \to K \to U$, $U \to E \to U$ and $U \to K \to U$ at the social layer.

The attributes of the social network are introduced into the IoT layer, and the status of the smart devices corresponding to individual users are divided into three categories: Susceptible (S), Infected (I), and Recovered (R). The specific meaning of each status of the smart device is given in Table II. The device follows the state transition rule of $S \to I \to R \to S$ at the IoT layer. The topology structure of each node in the IoT layer can

TABLE II
STATUS CLASSIFICATION OF SMART DEVICES IN THE IOT LAYER OF SIOT

Smart device status	Status name	Status meaning
S	Susceptible	The smart device has no information and can receive information from neighbor devices.
I	Infected	The smart device does receive the information and can forward it to a neighboring device.
R	Recovered	The smart device does receive the message, but has lost interest and no longer forwards it.

be point-to-point or centralized, and its topology structure may change with the change of communication requirements, but any topology structure will not affect the node status.

In the SIoT, coupled nodes are used to represent individual users within the social layer and smart devices within the IoT layer. According to the combination principle, from the divided social layer user individual status and the IoT layer smart device status, the coupling node has nine combined states, namely US (unknown-susceptible), UI (unknown-infected), UR (unknown-recovered), ES (exposed-susceptible), EI (exposed-infected), ER (exposed-recovered), KS (known-susceptible), KI (known-infected), and KR (known-recovered). However, in real life, UI and UR states do not exist, because if a US node receives information from smart devices from neighboring nodes, the devices will automatically transfer into the infected state, and individual users corresponding to the propagated devices will simultaneously be in the known or susceptible state, meaning that the UI state does not exist. Accordingly, the UR state does not exist either.

B. Cloud-edge Collaborative Dynamics Information Dissemination Model

According to the interaction mechanism of information dissemination between individual users in the social layer and smart devices in the IoT layer, a CCDIDM for SIoT is proposed, as shown in Fig. 2. The information dissemination process in the SIoT is described using this model. The transition probabilities shown between the coupling nodes within Fig. 2 are defined in Table III.

In Table III, when the node changes from US state to EI state or KI state, it can be considered that the state change in the IoT layer is from S state to I state in these two transformation processes. Since the Internet of Things layer enters the I state from the S state, then the state of the social layer will change from U state to E state or K state, so the transition probability of $US \to EI$ and $US \to KI$ is the same. In this paper, we set the probability of transition between $US \to EI$ and $US \to KI$ as β. Similarly, the transformation of $ES \to EI$ and $KS \to KI$ is only the state transformation in the IoT layer, and they are

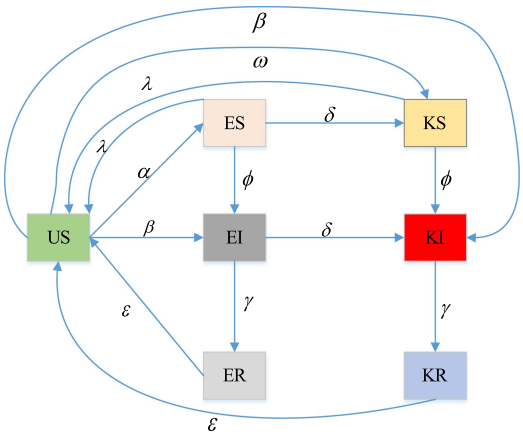

Fig. 2. Cloud-edge collaborative dynamics information dissemination model.

TABLE III
TRANSITION PROBABILITY BETWEEN COUPLED NODES IN THE CCDIDM MODEL

Symbol	Meaning
α	Probability that a US node is converted into an ES node
ω	Probability that a US node is converted into a KS node
β	Probability that a US node is converted into an EI node; Probability that a US node is converted into a KI node
ϕ	Probability that an ES node is converted into an EI node; Probability that a KS node is converted into a KI node
δ	Probability that an ES node is converted into a KS node; Probability that an EI node is converted into a KI node
γ	Probability that an EI node is converted into an ER node; Probability that a KI node is converted into a KR node
ε	Probability that an ER node is converted into a US node; Probability that a KR node is converted into a US node
λ	Probability that an ES node is converted into a US node Probability that a KS node is converted into a US node

both from S state to I state, so the transformation probability of $ES \rightarrow EI$ and $KS \rightarrow KI$ is the same as ϕ. In addition, the same is true for transition probabilities γ and ε.

When the node changes from ES state to KS state or EI state to KI state, it can be considered that there is only state transition in the social layer in these two transformation processes, and both of them change from E state to K state, so the transition probability of $ES \rightarrow KS$ and $EI \rightarrow KI$ is the same as δ. In addition, the same is true for transition probability λ.

Supposing that the sum number of coupled nodes in the CCDIDM, N, is constant, the information propagation process in the CCDIDM model is described as follows:

1) $US \rightarrow ES \rightarrow US$

When the US node receives information from the neighboring user, it is uncertain about the accuracy of the information and changes to the ES node with a probability of α. The ES node will become the US node with a probability of λ due to the forgetting behavior of individual users or their disinterest in transmitting information.

2) $US \rightarrow ES \rightarrow EI \rightarrow ER \rightarrow US$

When the US node receives information from the neighboring user, it becomes the ES node with a probability of α. After the ES node receives the information from the neighboring smart device, it becomes the EI state with a probability of ϕ. When the EI node judges that the information is inaccurate, it loses interest in the information, stops disseminating the information, and transforms into an ER node with a probability of γ. Some information deleted due to the failure of the smart device and other reasons, and ER node returns to the initial state with a probability of ε.

3) $US \rightarrow ES \rightarrow KS \rightarrow KI \rightarrow KR \rightarrow US$

When the US node receives information from the neighboring user, it becomes the ES node with a probability of α. When the ES node receives information from the neighboring nodes several times, it transforms into the KS node by the probability δ. After the KS node receives information from the neighboring smart device, it becomes KI state with a probability of ϕ. The KI node can transmit information to neighboring users and smart devices. When it is judged that the information is negative or useless, it loses interest in the information and stops dissemination, and becomes a KR node with a probability of γ. The KR node returns to the initial state with a probability of ε.

4) $US \rightarrow KS \rightarrow US$

When the US node receives information from the neighboring user, it determines the accuracy of the information and converts to the KS node with a probability of ω. Due to the forgetting behavior or disinterest of the individual user in the disseminated information, the KS node will become a US node with a probability of λ.

5) $US \rightarrow KS \rightarrow KI \rightarrow KR \rightarrow US$

After the US node receives information from the neighboring user, it will be converted to the KS node by the probability ω. When the KS node receives information from the neighboring smart device, it becomes the KI node with a probability of ϕ. The KI node can transmit information to neighboring users and smart devices. When it is judged that the information is false or useless, it loses interest in the information and stops dissemination, and becomes a KR node with a probability of γ. The KR node then will become the US node again by the probability ε.

6) $US \rightarrow EI \rightarrow ER \rightarrow US$

When the US node receives information from neighboring smart device, it cannot determine the accuracy of the information and converts to the EI node with a probability of β. The EI node then will convert to the ER node with a probability of γ.

The ER node finally becomes the US node again by the probability ε.

7) $US \rightarrow EI \rightarrow KI \rightarrow KR \rightarrow US$

After the US node receives information from the neighboring smart device, it becomes the EI node with a probability of β. When the EI node receives information from the neighboring nodes several times, it converts to the KI node with a probability of δ. The KI node then converts to the KR node with a probability of γ. The KR node finally becomes the US node again by the probability ε.

8) $US \rightarrow KI \rightarrow KR \rightarrow US$

When the US node receives information from the neighboring smart device, it determines the accuracy of the information and converts to the KI node with a probability of β. The KI node then converts to the KR node with a probability of γ. The KR node finally becomes the US node again by the probability ε.

The state changes of nodes at each layer need to follow the network architecture of the SIoT. Smart devices follow the state transition rules of $S \rightarrow I \rightarrow R \rightarrow S$ at the IoT layer, and individual users follow the state transition rules of $U \rightarrow E \rightarrow K \rightarrow U$, $U \rightarrow E \rightarrow U$ and $U \rightarrow K \rightarrow U$ at the social layer. Combined with the practical significance of each state, it can be seen that each state must strictly abide by the rules of state transition, and cross-state transformation and reverse transformation cannot be allowed. For example, in the $I \rightarrow S$ process of the IoT layer, it needs to go through the $I \rightarrow R$ and $R \rightarrow S$ process respectively, because the smart device in the spreading state needs to go through the process of losing interest in the current information before it can be transformed into the sensitive state without information in the smart device. In addition, the coupled two-layer network still follows the rules of state transition of the IoT layer and the social layer.

Based on the above node conversion relationships, the dynamic differential form of the CCDIDM for the SIoT is shown in (1), shown at the bottom of the page, where,

$$\begin{aligned} &US(t) + ES(t) + EI(t) + ER(t) + KS(t) \\ &\quad + KI(t) + KR(t) = 1 \end{aligned} \tag{2}$$

The initial conditions of each type of node in the network at the start of information dissemination are: $0 < US(0) \leq 1, 0 \leq ES(0) < 1,\ 0 \leq EI(0) < 1,\ 0 \leq ER(0) < 1,\ 0 \leq KS(0) < 1,\ 0 \leq KI(0) < 1,\ 0 \leq KR(0) < 1$.Due to the limited computing capacity of smart devices in the IoT layer, local edge devices or cloud servers can be used for computing processing when computing tasks are required [27], [28]. When the computing task is processed by the cloud server, there is a delay, and individual users cannot immediately receive the processed information. However, if the computing task is processed by the edge device, the individual user will receive a timely response, and this will improve the perception of the information.

As shown in Fig. 2, after receiving the information of the neighboring smart device, the US node is transformed into the EI and KI nodes with a probability of β, and this is regarded as the cloud processing the information of the smart device. Simultaneously, after receiving the information from the neighboring smart device, the ES node and KS node are transformed into the EI and KI nodes with a probability of ϕ. This is the process in which the information of the smart device is processed by the local edge device. As the time of feedback of the result to the individual user after processing the computing task from the local edge device is faster than that from the cloud server, the individual user has a stronger sense of information and is more likely to know the information transmitted by the smart device. In addition, the interaction between individual users in social networks will have an impact on the dissemination of information between smart devices. Individual users with strong perception will inhibit the information dissemination of smart devices, and thus $\phi < \beta$. Considering the different perceptions of individual users, we define ϕ as follows:

$$\phi = (1/z)^{\sigma}\beta \tag{3}$$

where, z is the perceptual awareness of the individual user. The larger z is, the stronger the individual users' perception awareness is, and stronger the inhibition effect of individual users on the information transmission of smart devices is. σ is defined as the adjustment parameter of the perceptual awareness of the individual user.

III. Model Dynamics Analysis

Investigating the dynamic characteristics of the CCDIDM for SIoT is of great significance for effectively predicting and controlling information diffusion. Therefore, in this section, we analyze the dynamic characteristics of the CCDIDM, including the equilibrium point, threshold, and its stability.

A. Equilibrium Points and Threshold

As information spreads in the SIoT, *US(t), ES(t), EI(t), ER(t), KS(t), KI(t),* and *KR(t)* change over time. When the proportionality of the nodes in the seven states no longer changes, the network is known to have reached equilibrium. In order to solve the equilibrium point of the CCDIDM, let us define the derivative

$$\begin{cases} \frac{dUS(t)}{dt} = -(\alpha+\omega+2\beta)KI(t)US(t) + \varepsilon ER(t) + \varepsilon KR(t) + \lambda ES(t) + \lambda KS(t) \\ \frac{dES(t)}{dt} = \alpha KI(t)US(t) - \phi KI(t)ES(t) - \delta ES(t) - \lambda ES(t) \\ \frac{dEI(t)}{dt} = \beta KI(t)US(t) + \phi KI(t)ES(t) - \delta EI(t) - \gamma EI(t) \\ \frac{dER(t)}{dt} = -\varepsilon ER(t) + \gamma EI(t) \\ \frac{dKS(t)}{dt} = \omega KI(t)US(t) + \delta ES(t) - \phi KI(t)KS(t) - \lambda KS(t) \\ \frac{dKI(t)}{dt} = \beta KI(t)US(t) + \phi KI(t)KS(t) + \delta EI(t) - \gamma KI(t) \\ \frac{dKR(t)}{dt} = -\varepsilon KR(t) + \gamma KI(t) \end{cases} \tag{1}$$

of each state with respect to time to be 0, i.e., $\frac{di}{dt} = 0$, where $i =$ *US(t), ES(t), EI(t), ER(t), KS(t), KI(t),* and *KR(t).* By doing so, (1) can be written as shown in (4) at the bottom of the page.

Solving (4) obtains two equilibrium points in the CCDIDM, i.e., the information-free equilibrium point $E^0 = (1, 0, 0, 0, 0, 0, 0)$ and the information equilibrium point $E^* = (US^*, ES^*, EI^*, ER^*, KS^*, KI^*, KR^*)$.

Theorem 1: Assume that R_0 is the dissemination threshold of the CCDIDM. Then, $R_0 = \rho(FV^{-1}) = \frac{\delta\beta+(\delta+\gamma)\beta}{\gamma(\delta+\gamma)}$.

Proof: See Appendix A.

B. Stability Analysis of Equilibrium Points

Theorem 2: When $R_0 < 1$, the information-free equilibrium point E^0 is locally asymptotically stable. Where $R_0 > 1$, E^0 is unstable.

Proof: See Appendix B.

Theorem 3: When $R_0 < 1$, the information-free equilibrium point E^0 of the CCDIDM is globally asymptotically stable.

Proof: See Appendix C.

Theorem 3: When $R_0 > 1$, the information equilibrium point E^* of the CCDIDM is globally asymptotically stable.

Proof: See Appendix D.

IV. Simulation Results and Analysis

In this section, the stability of information dissemination and the influence of the dissemination mechanism are verified through numerical simulations. The specific simulation results and analysis are as follows.

In reality, the behavior of individual users and the resetting or communication interruption of IoT smart devices will have a certain impact on information dissemination in SIoT networks. This section explores the influence of different dissemination mechanisms on the scale of information dissemination. Due to the limitation of computing power, most edge devices in the cloud-edge collaborative SIoT only have a small number of connections, and its topological network structure is scale-free. That means the degree of nodes follows the power-law distribution, with most nodes having a small degree and a few nodes having a large degree. Therefore, this paper constructs a Barabási–Albert (BA) scale-free network with 1000 nodes to conduct subsequent simulation experiments.

A. Stability Verification of Information Dissemination

This paper simulates the process of information dissemination in the CCDIDM by setting different parameters that ensure the information dissemination thresholds $R_0 < 1$ and $R_0 > 1$ are satisfied. The stability of information dissemination is verified by analyzing the trend of the proportion of various types of nodes in the model as a function of time.

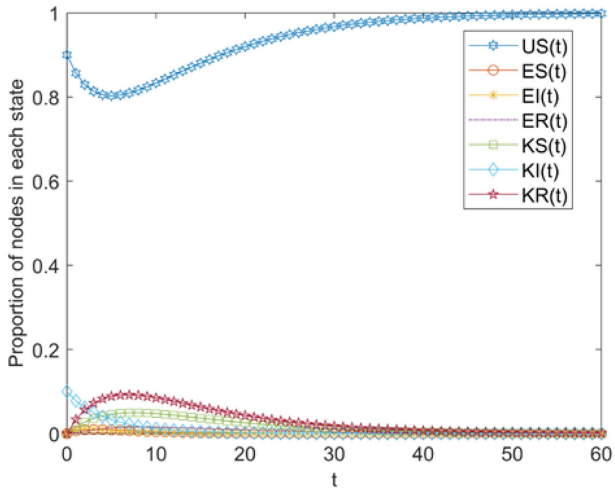

Fig. 3. The change in the proportion of various types of nodes in the cloud-edge collaborative dynamic information dissemination model when $R_0 < 1$.

1) Case 1: $R_0 < 1$

Set the parameters $\alpha = 0.1$, $\omega = 0.2$, $\beta = 0.15$, $\varepsilon = 0.1$, $\lambda = 0.1$, $\delta = 0.3$, $\gamma = 0.4$, $z = 2.7$, and $\sigma = 0.5$, and set the initial proportion of each type of node in the network to be $US(0) = 0.9, KI(0) = 0.1, ES(0) = 0, KS(0) = 0, EI(0) = 0$, $ER(0) = 0$, and $KR(0) = 0$. According to Theorem 1, we achieve $R_0 \approx 0.536 < 1$. The simulation results of the proportion of each type of node changing with time are shown in Fig. 3.

In Fig. 3, the horizontal axis represents the time of information dissemination, and the vertical axis represents the proportion of all types of nodes within the network. The proportional change of each state are represented by the blue solid line with six-pointed stars, the orange solid line with circles, the yellow solid line with asterisks, the purple dotted line, green solid line with squares, the light blue solid line with diamonds, and the red solid line with five-pointed stars, respectively. It is clear from Fig. 3 that the proportions of the seven state nodes in the network eventually tend to be stable over time. Specifically, proportion of US nodes gradually approaches 1, while the number of other nodes gradually approaches 0. At this point, the system reaches stability. The KI node in the SIoT network disappears, and the information will not spread, forming an equilibrium point of no information dissemination, which is consistent with the theoretical analysis result of Theorem 1.

$$\begin{cases} -(\alpha+\omega+2\beta)\,KI(t)\,US(t)+\varepsilon ER(t)+\varepsilon KR(t)+\lambda ES(t)+\lambda KS(t)=0 \\ \alpha KI(t)\,US(t)-\phi KI(t)\,ES(t)-\delta ES(t)-\lambda ES(t)=0 \\ \beta KI(t)\,US(t)+\phi KI(t)\,ES(t)-\delta EI(t)-\gamma EI(t)=0 \\ -\varepsilon ER(t)+\gamma EI(t)=0 \\ \omega KI(t)\,US(t)+\delta ES(t)-\phi KI(t)\,KS(t)-\lambda KS(t)=0 \\ \beta KI(t)\,US(t)+\phi KI(t)\,KS(t)+\delta EI(t)-\gamma KI(t)=0 \\ -\varepsilon KR(t)+\gamma KI(t)=0 \end{cases} \tag{4}$$

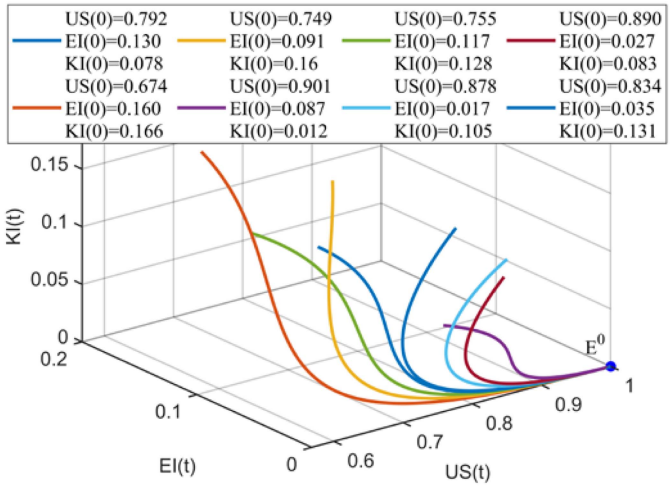

Fig. 4. Stability of the information-free equilibrium point at different initial proportions.

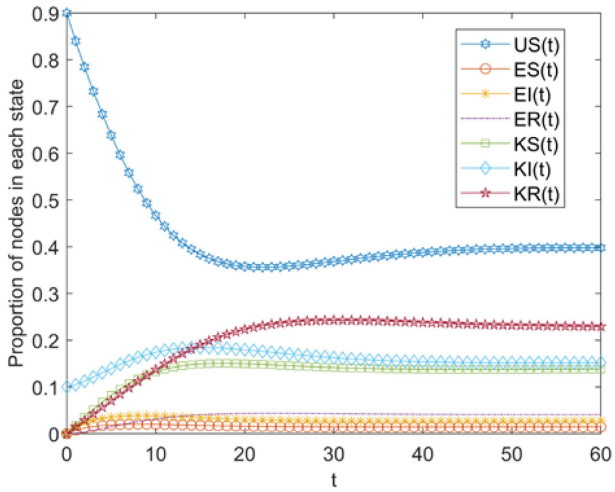

Fig. 5. The change in the proportion of various types of nodes in the cloud-edge collaborative dynamic information dissemination model when $R_0 > 1$.

In addition, by randomly setting the initial proportion of each state node, the CCDIDM can achieve dynamic equilibrium, as shown in Fig. 4. Here, x-axis represents the proportion of US nodes, y-axis represents the proportion of EI nodes, and z-axis represents the proportion of KI nodes. The curves of different colors in the figure represent the changes in the number of US, EI, and KI nodes with time under different initial proportions chosen randomly for the different types of nodes. It is clear from Fig. 4 that the proportional trajectory curves of the US, EI, and KI nodes eventually converge at the information-free equilibrium point E^0, and the system is therefore stable.

2) Case 2: $R_0 > 1$

In this case, we set the parameters as $\alpha = 0.1, \omega = 0.2, \beta = 0.2, \varepsilon = 0.1, \lambda = 0.1, \delta = 0.3, \gamma = 0.15, z = 2.7$, and $\sigma = 0.5$, and the initial proportion of each type of node in the network is set to be $US(0) = 0.9, KI(0) = 0.1, ES(0) = 0, KS(0) = 0, EI(0) = 0, ER(0) = 0$, and $KR(0) = 0$. According to (14), we achieve $R_0 \approx 2.22 > 1$. The simulation results of the proportion of each type of node changing with time are shown in Fig. 5. The legend in Fig. 5 is consistent with Fig. 3.

Fig. 5 shows that the proportions of nodes in the seven states tend to be stable after a period of time. Specifically, the proportion of each state gradually approached 0.40, 0.01, 0.03, 0.04, 0.14, 0.15, and 0.23, respectively. At this point, the system reaches a steady state, forming an equilibrium point of information dissemination, and the information then continues to be disseminated stably in the SIoT network.

In addition, by randomly setting the initial proportion of each state node, the CCDIDM can also achieve dynamic equilibrium, as shown in Fig. 6. The meaning of x, y and z axis in Fig. 6 is the same as that in Fig. 4. The curves of different colors in the figure represent the changes of the number of US, EI, and KI nodes with time under different initial proportions determined randomly by different types of nodes. It is clear from Fig. 6 that the proportional trajectory curves of the US, EI, and KI nodes eventually converge at the information equilibrium point E^*, and

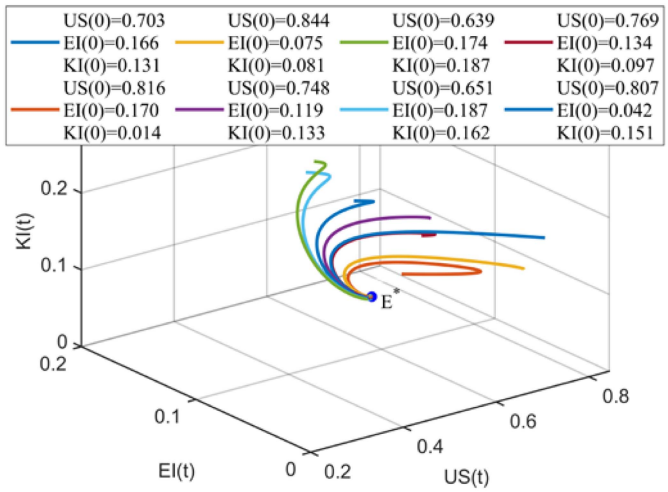

Fig. 6. Stability of the information-free equilibrium point at different initial proportions.

the system becomes stable. Therefore, this is consistent with the theoretical analysis results.

B. Analysis of the Influence of Dissemination Mechanism on Information Dissemination

First, we set the parameters as $\alpha = 0.1, \omega = 0.2, \beta = 0.2, \varepsilon = 0.1, \lambda = 0.1, \delta = 0.3, \gamma = 0.15$, and $\sigma = 0.5$, Due to the practical significance of these parameters, their values are all between $[0, 1]$. We set the initial proportion of the seven state nodes is set to be $US(0) = 0.9, KI(0) = 0.1, ES(0) = 0, KS(0) = 0, EI(0) = 0, ER(0) = 0$, and $KR(0) = 0$[34], [35], [36]. By changing the setting of the user's individual perception awareness z, the influence of perception awareness on information dissemination can be analyzed. We set the values of z to be 1, 2.7, 4, 6, and 9, and investigated the change of KI nodes with time. The simulation results are shown in Fig. 7.

Here, the horizontal axis represents the time of information dissemination, and the vertical axis represents the proportion

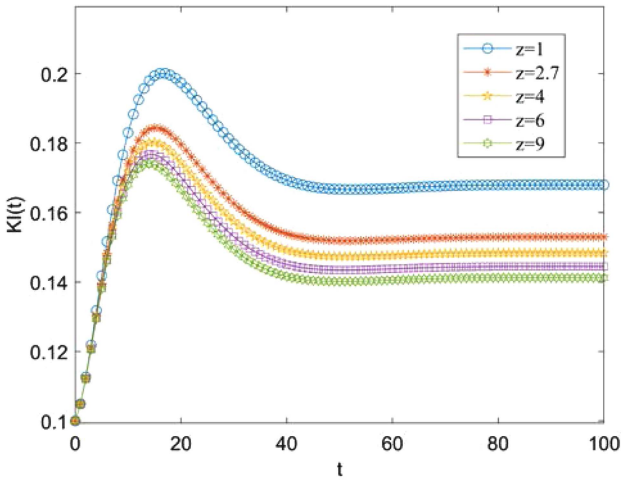

Fig. 7. Influence of user's individual perception awareness on information dissemination.

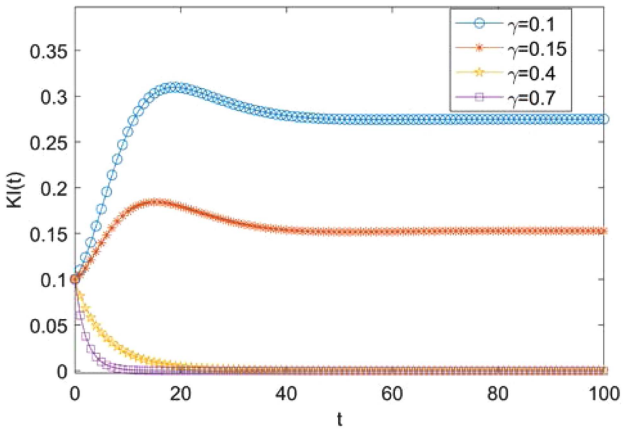

Fig. 8. Influence of parameter γ on information dissemination.

of KI nodes within the network. The solid lines with circles, asterisks, five-pointed stars, squares, and six-pointed stars are the simulated values of the proportion of KI nodes in the network when the perception awareness is 1, 2.7, 4, 6, and 9, respectively. It is clear from Fig. 7 that when the perceptual awareness of individual users is different, the change in the number of KI nodes with time first increases to the peak value, then decreases, and finally tends toward stability. As z increases, the number of KI nodes gradually decreases. This shows that the interaction between individual users under the cloud-edge collaboration reduces the possibility of information dissemination. When individual users have a stronger sense of perception, the spread of interactive behavior is conducive to the control of the dissemination of information.

Second, we varied the parameter γ to analyze its influence on information dissemination. We set the values of γ to be 0.1, 0.15, 0.4, and 0.7, and studied the change in the number of KI nodes with time. The simulation results are shown in Fig. 8, where the solid lines with circles, asterisks, five-pointed stars, and squares represent the simulated values of the proportion of KI nodes within the network when γ is 0.1, 0.15, 0.4, and 0.7, respectively.

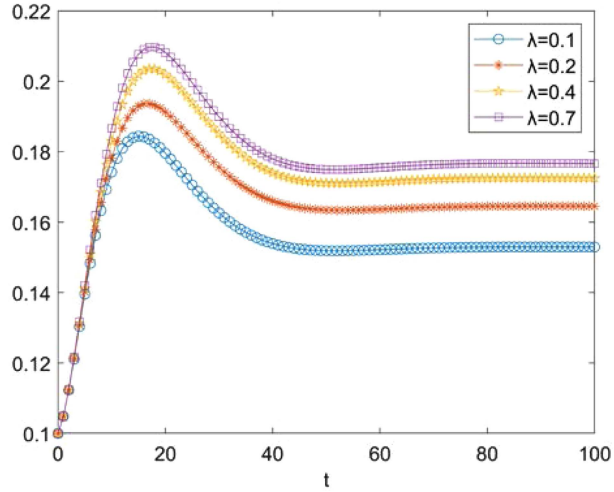

Fig. 9. Influence of parameter λ on information dissemination.

Fig. 8 shows that when γ is 0.1 and 0.15, the number of KI nodes first increases and then decreases, and then tends toward stability. Information will then propagate steadily in the network, because the network propagation threshold is greater than 1. When γ is 0.4 and 0.7, the number of KI nodes in the network decreases with time, reaching a final value of 0. This is because increasing the value of γ results in the network propagation threshold being less than 1, and the propagation nodes in the network eventually disappear. This shows that the parameter γ affects the scale of information propagation. In addition, it can also be seen that the larger γ is, the shorter the time required for the network to reach stability.

Next, we varied the parameter λ to analyze its influence on information dissemination. We set the values of λ to be 0.1, 0.2, 0.4, and 0.7, and the influences of different values of λ on the propagation nodes can be seen in Fig. 9.

In Fig. 9, the solid lines with circles, asterisks, five-pointed stars, and squares represent the simulated values of the proportion of KI nodes in the network when λ is 0.1, 0.2, 0.4, and 0.7, respectively. Fig. 9 shows that when the value of λ varies, the proportion of KI nodes in the network first increases and then decreases with time, and finally tends toward stability. Furthermore, as the parameter λ increases, the number of KI nodes in the network also increases. This shows that the parameter λ has an influence on the evolution process of the CCDIDM and will affect the dissemination scale.

In addition, the influence of parameter ε on information propagation was also analyzed. We set the values of ε to be 0.1, 0.2, 0.4, and 0.7, and the influence of different values of ε on the proportion of KI nodes is shown in Fig. 10.

In Fig. 10, the solid lines with circles, asterisks, five-pointed stars, and squares represent the simulated values of the proportion of KI nodes in the network when ε is 0.1, 0.2, 0.4, and 0.7, respectively. Fig. 10 demonstrates that even when ε takes different values, the number of KI nodes tends to be stable after a period of time. As ε increases, the proportion of KI nodes in the network also increases. This shows that the parameter ε affects the scale of information dissemination in the SIoT network.

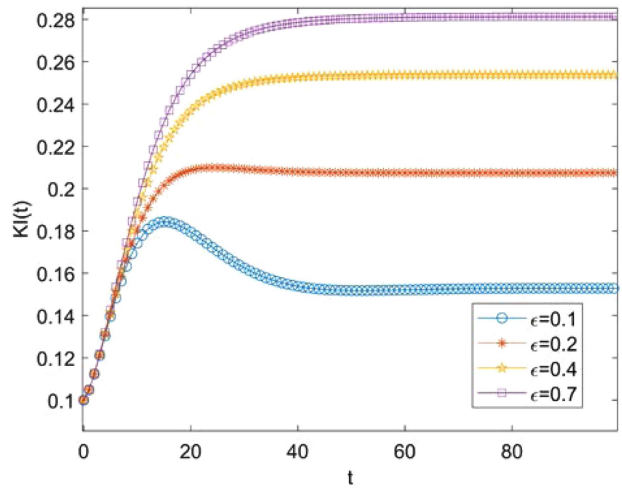

Fig. 10. Influence of parameter ε on information dissemination.

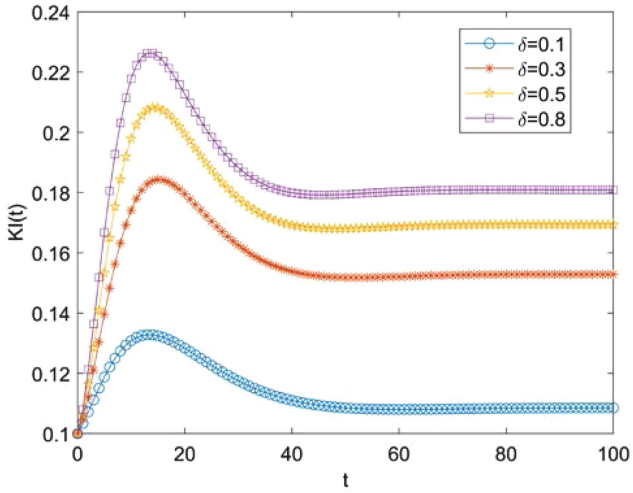

Fig. 11. Influence of parameter δ on information dissemination.

We verified the influence of the parameter δ on information dissemination. Simulation results for different values of δ are shown in Fig. 11. In Fig. 11, the solid lines with circles, asterisks, five-pointed stars, and squares represent the simulated values of the proportion of KI nodes in the network when δ is 0.1, 0.3, 0.5, and 0.8, respectively. Fig. 11 shows that, as δ increases from 0.1 to 0.8, the number of KI nodes tends to a constant value at a faster rate. Varying the parameter δ also affects the scale of information dissemination.

Based on the above analysis, we can deduce that when the dissemination threshold $R_0 < 1$ and $R_0 > 1$, the cloud-edge cooperative info rmation dissemination system will be stable at the equilibrium point. In addition, by adjusting the parameters z, γ, λ, ε and δ, different scales of information dissemination can be obtained, thereby inhibiting or promoting the dissemination of information.

Finally, the proportion of each state node of the cloud edge collaborative dynamics information dissemination model(model B) for social Internet of Things and the coupled dynamics information dissemination model(model A) without considering

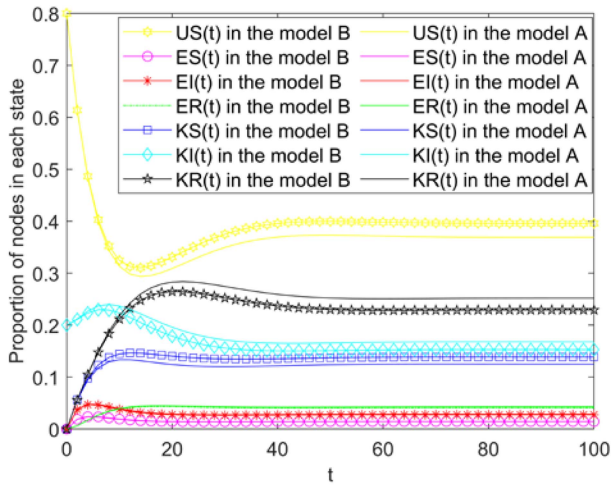

Fig. 12. Influence of parameter δ on information dissemination.

the cloud edge collaboration SIOT architecture are compared through experiments to verify the effectiveness of the proposed model. The parameter $\alpha = 0.1$, $\omega = 0.2$, $\beta = 0.2$, $\phi = 0.2$, $\varepsilon = 0.1$, $\lambda = 0.1$, $\delta = 0.3$, $\gamma = 0.15$ of the coupling dynamic information propagation model A under the cloud edge cooperative SIOT architecture and the initial proportion $US(0) = 0.8$, $KI(0) = 0.2$, $ES(0) = 0$, $KS(0) = 0$, $EI(0) = 0$, $ER(0) = 0$, $KR(0) = 0$ of each type of nodes in the network are set. The simulation results are shown in Fig. 12.

In the Fig. 12, the abscissa is the time of information transmission, and the ordinate is the proportion of various nodes in the network. As can be seen from Fig. 12, the number of US nodes, ES nodes and KS nodes in the cloud edge cooperative information propagation model is more than that in the coupled dynamics information propagation model under the SIOT architecture, while the number of EI nodes, KI nodes, ER nodes and KR nodes is opposite. This is because cloud-edge collaborative computing can bring feedback to nodes and further improve their social perception. When there are subjective judgments and social interactions, nodes will interfere with information dissemination. Therefore, there are many KI propagation nodes in the information propagation model of coupling dynamics under SIOT architecture.

V. Conclusion

In this study, we investigated the problem of information dissemination in the Social Internet of Things (SIoT), and we proposed CCDIDM for the SIoT. The model first considers both the interaction between individual users and the interactive influence of information dissemination between IoT devices, and subsequently establishes the relationship of information dissemination between coupled nodes. Subsequently, considering that both the real-time processing and the result feedback of cloud-edge computing have different information cognition awareness for users, a corresponding communication mechanism relationship is established to realize the efficient interactive communication of information. The information dissemination threshold of the CCDIDM is deduced through theoretical

analysis, and the stability of the equilibrium point is analyzed through LaSalle's invariance and the Lyapunov method. Finally, we verified the stability of CCDIDM and analyzed the influence of different dissemination mechanisms on information dissemination through simulation experiments. The simulation results showed that the system is stable at the equilibrium point. The perception awareness of individual users under cloud-edge collaboration affects the dissemination scale of information. Stronger the perception awareness of individual users, smaller the scale of information dissemination. In addition, adjusting the propagation mechanism parameters such as γ, λ, ε, and δ within the model will also inhibit or promote the diffusion of information and affect the scale of information dissemination. The model proposed in this paper can provide theoretical guidance for information dissemination control and prediction in Social Internet of Things scenarios.

In the future research work, the correlation between different communication factors and the security mechanism in the IoT layer will be considered to analyze the information dissemination in the SIoT. In addition, the delay difference between edge side processing and cloud side processing will be analyzed for the proposed network, and then its impact on information transmission will be studied.

Appendix A
Proof of Theorem 1

In order to acquire the dissemination threshold of the CCDIDM, the basic reproduction number of (1) can be obtained using the regeneration matrix method [29], [30], [31], which is the information dissemination threshold R_0.

If we define

$$\chi = (KI(t), EI(t), KS(t), ES(t), US(t), KR(t), ER(t))^T \tag{5}$$

(1) can be written as

$$\frac{d\chi}{dt} = F(\chi) - V(\chi) \tag{6}$$

where,

$$V(\chi) = V^-(\chi) - V^+(\chi) \tag{7}$$

$F(\chi)$ indicates the new rate of infected nodes among the seven state nodes; $V(\chi)$ indicates the transition rate of seven state nodes; $V^-(\chi)$ is the rate at which this state node becomes another node; $V^+(\chi)$ is the rate at which other node becomes this state node. Therefore, $F(\chi)$ and $V(\chi)$ can be expressed as

$$F(\chi) = \begin{pmatrix} \beta KI(t)US(t) + \phi KI(t)KS(t) \\ \beta KI(t)US(t) + \phi KI(t)ES(t) \\ \omega KI(t)US(t) \\ \alpha KI(t)US(t) \\ 0 \\ 0 \\ 0 \end{pmatrix} \tag{8}$$

and (9), shown at the bottom of the page.

The Jacobian matrix of $F(\chi)$ and $V(\chi)$ at the information-free equilibrium point E^0 can be expressed as

$$DF(E^0) = \begin{pmatrix} F & 0 \\ 0 & 0 \end{pmatrix}, DV(E^0) = \begin{pmatrix} V & 0 \\ J_1 & J_2 \end{pmatrix} \tag{10}$$

where,

$$F = \left[\frac{\partial F_i}{\partial \chi_y}(E^0)\right], V = \left[\frac{\partial V_i}{\partial \chi_y}(E^0)\right] \; 1 \le i, y \le 4 \tag{11}$$

By substituting (8) and (9) into (11), the following can be obtained

$$\begin{cases} F = \begin{bmatrix} \beta & 0 & 0 & 0 \\ \beta & 0 & 0 & 0 \\ \omega & 0 & 0 & 0 \\ \alpha & 0 & 0 & 0 \end{bmatrix} \\ V = \begin{bmatrix} \gamma & -\delta & 0 & 0 \\ 0 & \delta+\gamma & 0 & 0 \\ 0 & 0 & \lambda & -\delta \\ 0 & 0 & 0 & \delta+\lambda \end{bmatrix} \end{cases} \tag{12}$$

According to (12), the regeneration matrix FV^{-1} can be obtained as follows

$$FV^{-1} = \begin{bmatrix} \frac{\beta}{\gamma} & \frac{\delta\beta}{\gamma(\delta+\gamma)} & 0 & 0 \\ \frac{\beta}{\gamma} & \frac{\delta\beta}{\gamma(\delta+\gamma)} & 0 & 0 \\ \frac{\omega}{\gamma} & \frac{\delta\omega}{\gamma(\delta+\gamma)} & 0 & 0 \\ \frac{\alpha}{\gamma} & \frac{\delta\alpha}{\gamma(\delta+\gamma)} & 0 & 0 \end{bmatrix} \tag{13}$$

Therefore, the information dissemination threshold of the CCDIDM is defined as

$$R_0 = \rho(FV^{-1}) = \frac{\delta\beta + (\delta+\gamma)\beta}{\gamma(\delta+\gamma)} \tag{14}$$

Appendix B
Proof of Theorem 2

According to (1), the Jacobian matrix of the CCDIDM can be expressed by (15), shown at the bottom of the next page.

Therefore, the characteristic equation of the Jacobian matrix $J(E_0)$ of the CCDIDM at the information-free equilibrium point

$$V(\chi) = \begin{pmatrix} \gamma KI(t) - \delta EI(t) \\ (\delta+\gamma)EI(t) \\ \phi KI(t)KS(t) - \delta ES(t) + \lambda KS(t) \\ \phi KI(t)ES(t) + \delta ES(t) + \lambda ES(t) \\ (\alpha+\omega+2\beta)KI(t)US(t) - \varepsilon KR(t) - \varepsilon ER(t) - \lambda KS(t) - \lambda ES(t) \\ \varepsilon KR(t) - \gamma KI(t) \\ \varepsilon ER(t) - \gamma EI(t) \end{pmatrix} \tag{9}$$

E^0 is expressed as (16), shown at the bottom of this page, where $I_{7\times7}$ is the 7th order identity matrix.

By solving (16), the characteristic roots can be obtained, as shown in (17).

$$\begin{cases} \rho_1 = \rho_2 = -\varepsilon \\ \rho_3 = -\lambda \\ \rho_4 = -\lambda - \delta \\ \rho_5 = \frac{\beta}{2} - \frac{\delta}{2} - \gamma - \frac{\left(\beta^2+6\beta\delta+\delta^2\right)^{1/2}}{2} \\ \rho_6 = \frac{\beta}{2} - \frac{\delta}{2} - \gamma + \frac{\left(\beta^2+6\beta\delta+\delta^2\right)^{1/2}}{2} \end{cases} \tag{17}$$

When $R_0 < 1$, we acquire $\beta < \gamma$. Therefore,

$$\rho_5 = \frac{\beta}{2} - \frac{\delta}{2} - \gamma - \frac{\left(\beta^2 + 6\beta\delta + \delta^2\right)^{1/2}}{2} < 0.$$

From ρ_5 and ρ_6, the following can be obtained:

$$\rho_5\rho_6 = \frac{4\gamma(\delta+\gamma) - 4\beta(2\delta+\gamma)}{4} \tag{18}$$

When $R_0 < 1$, we acquire $\rho_5\rho_6 > 0$ and $\rho_6 < 0$.

Therefore, when $R_0 < 1$, all characteristic roots are negative. By the Hurwitz stability criterion, the system is locally asymptotically stable at the information-free equilibrium point.

When $R_0 > 1$, not all of the characteristic roots of the Jacobi matrix at the information-free equilibrium point E^0 are negative. The Hurwitz stability criterion demonstrates that the system is unstable at the information-free equilibrium point E^0.

Appendix C
Proof of Theorem 3

In order to study the global asymptotic stability of the CCDIDM at the information-free equilibrium point E^0, a Lyapunov function is constructed, as shown in (19).

$$L(t) = EI(t) + \mu_1 KI(t) \tag{19}$$

By combining this with (1), the derivative of $L(t)$ can be obtained, as shown in (20).

$$\begin{aligned} \frac{dL(t)}{dt} &= \frac{dEI(t)}{dt} + \mu_1\frac{dKI(t)}{dt} \\ &= \beta KI(t)\left[1 - ES(t) - EI(t) - ER(t) - KI(t)\right. \\ &\quad \left. -KS(t) - KR(t)\right] \\ &\quad + \phi KI(t)ES(t) - \delta EI(t) - \gamma EI(t) \\ &\quad + \mu_1\left[\beta KI(t)(1 - ES(t) - EI(t) - ER(t)\right. \\ &\quad \left. -KI(t) - KS(t) - KR(t)\right) \\ &\quad \left. +\phi KI(t)KS(t) + \delta EI(t) - \gamma KI(t)\right] \\ &= (\beta+\mu_1\beta - \mu_1\gamma)KI(t) - (\beta - \phi + \mu_1\beta)KI(t)ES(t) \\ &\quad - (\beta+\mu_1\beta)KI(t)EI(t) - (\beta + \mu_1\beta)KI(t)ER(t) \\ &\quad - (\beta+\mu_1\beta - \mu_1\phi)KI(t)KS(t) - (\beta+\mu_1\beta)KI^2(t) \\ &\quad - (\beta + \mu_1\beta)KI(t)KR(t) - (\delta + \gamma - \delta\mu_1)EI(t) \end{aligned} \tag{20}$$

Taking $\mu_1 = \frac{\delta+\gamma}{\delta}$, we get:

$$\beta + \mu_1\beta - \mu_1\gamma = \frac{2\delta+\gamma}{\delta}\beta - \frac{(\delta+\gamma)\gamma}{\delta}. \tag{21}$$

When $R_0 < 1$, we acquire $(2\delta+\gamma)\beta < (\delta+\gamma)\gamma$. From this, it can be seen that $\beta + \mu_1\beta - \mu_1\gamma < 0$.

In addition, from $\beta > \phi$, we can get $\beta - \phi + \mu_1\beta > 0$ and $\beta + \mu_1\beta - \mu_1\phi > 0$.

Therefore, for $\forall\mu_1 > 0$, $\frac{dL(t)}{dt} \le 0$, and $\frac{dL(t)}{dt} = 0$ if and only if $E^0 == (1,0,0,0,0,0,0)$. According to the LaSalle's invariance principle, the information-free equilibrium point of the CCDIDM is globally asymptotically stable for $R_0 < 1$.

$$J = \begin{bmatrix} -(\alpha+\omega+2\beta)KI(t) & \lambda & 0 & \varepsilon & \lambda & -(\alpha+\omega+2\beta)US(t) & \varepsilon \\ \alpha KI(t) & -\phi KI(t) - \delta - \lambda & 0 & 0 & 0 & \alpha US(t) - \phi ES(t) & 0 \\ \beta KI(t) & \phi KI(t) & -\delta - \gamma & 0 & 0 & \beta US(t) + \phi ES(t) & 0 \\ 0 & 0 & \gamma & -\varepsilon & 0 & 0 & 0 \\ \omega KI(t) & \delta & 0 & 0 & -\phi KI(t) - \lambda & \omega US(t) - \phi KS(t) & 0 \\ \beta KI(t) & 0 & \delta & 0 & \phi KI(t) & \beta US(t) + \phi KS(t) - \gamma & 0 \\ 0 & 0 & 0 & 0 & 0 & \gamma & -\varepsilon \end{bmatrix} \tag{15}$$

$$\det(\rho I_{7\times7} - J(E_0)) = \begin{vmatrix} \rho & \lambda & 0 & \varepsilon & \lambda & -(\alpha+\omega+2\beta) & \varepsilon \\ 0 & \rho+\delta+\lambda & 0 & 0 & 0 & \alpha & 0 \\ 0 & 0 & \rho+\delta+\gamma & 0 & 0 & \beta & 0 \\ 0 & 0 & \gamma & \rho+\varepsilon & 0 & 0 & 0 \\ 0 & \delta & 0 & 0 & \rho+\lambda & \omega & 0 \\ 0 & 0 & \delta & 0 & 0 & \rho-\beta+\gamma & 0 \\ 0 & 0 & 0 & 0 & 0 & \gamma & \rho+\varepsilon \end{vmatrix} = 0 \tag{16}$$

APPENDIX D
PROOF OF THEOREM 4

Firstly, the information equilibrium point E^* satisfies (1). Therefore, (22) can be obtained, as follows:

$$\begin{cases} -(\alpha+\omega+2\beta)KI^*US^*+\varepsilon ER^*+\varepsilon KR^*+\lambda ES^*+\lambda KS^*=0 \\ \alpha KI^*US^* - \phi KI^*ES^* - \delta ES^* - \lambda ES^* = 0 \\ \beta KI^*US^* + \phi KI^*ES^* - \delta EI^* - \gamma EI^* = 0 \\ -\varepsilon ER^* + \gamma EI^* = 0 \\ \omega KI^*US^* + \delta ES^* - \phi KI^*KS^* - \lambda KS^* = 0 \\ \beta KI^*US^* + \phi KI^*KS^* + \delta EI^* - \gamma KI^* = 0 \\ -\varepsilon KR^* + \gamma KI^* = 0 \end{cases} \tag{22}$$

Then, we construct a Lyapunov function, as shown in (23). By letting $x_1 = \frac{US(t)}{US*}$, $y_1 = \frac{ES(t)}{ES*}$, $y_2 = \frac{EI(t)}{EI^*}$, $y_3 = \frac{ER(t)}{ER^*}$, $z_1 = \frac{KS(t)}{KS*}$, $z_2 = \frac{KI(t)}{KI^*}$, and $z_3 = \frac{KR(t)}{KR^*}$, the derivative of $L(t)$ is can be defined as in (24).

$$\begin{aligned} L(t) = {} & AUS*g\left(\frac{US(t)}{US*}\right) + BKI^*g\left(\frac{KI(t)}{KI^*}\right) \\ & + CKR^*g\left(\frac{KR(t)}{KR^*}\right) + ES*g\left(\frac{ES(t)}{ES*}\right) \\ & + EI^*g\left(\frac{EI(t)}{EI^*}\right) + ER^*g\left(\frac{ER(t)}{ER^*}\right) \\ & + KS*g\left(\frac{KS(t)}{KS*}\right) \end{aligned} \tag{23}$$

where $g(x) = x - 1 - \ln x$. When $x > 0$, we get $g(x) \geq 0$. A, B and C are all constants greater than 0.

$$\begin{aligned} \frac{dL(t)}{dt} = {} & A\left(1-\frac{1}{x_1}\right)\frac{dUS(t)}{dt} + B\left(1-\frac{1}{z_2}\right)\frac{dKI(t)}{dt} \\ & + C\left(1-\frac{1}{z_3}\right)\frac{dKR(t)}{dt} \\ & + \left(1-\frac{1}{y_1}\right)\frac{dES(t)}{dt} + \left(1-\frac{1}{y_2}\right)\frac{dEI(t)}{dt} \\ & + \left(1-\frac{1}{y_3}\right)\frac{dER(t)}{dt} + \left(1-\frac{1}{z_1}\right)\frac{dKS(t)}{dt} \end{aligned} \tag{24}$$

Combining (1) and (22), we get the following:

$$\begin{aligned} \frac{dUS(t)}{dt} = {} & -(\alpha+\omega+2\beta)(KI(t)US(t) - KI^*US*) \\ & + \varepsilon(ER(t) - ER^*) + \varepsilon(KR(t) - KR^*) \\ & + \lambda(ES(t) - ES^*) + \lambda(KS(t) - KS^*) \\ = {} & -(\alpha+\omega+2\beta)KI^*US*(x_1z_2 - 1) \\ & + \varepsilon ER^*(y_3 - 1) \\ & + \varepsilon KR^*(z_3 - 1) + \lambda ES^*(y_1 - 1) + \lambda KS^*(z_1 - 1) \end{aligned} \tag{25}$$

$$\begin{aligned} \frac{dES(t)}{dt} = {} & \alpha(KI(t)US(t) - KI^*US*) \\ & - \phi(KI(t)ES(t) - KI^*ES^*) \\ & - (\delta+\lambda)(ES(t) - ES^*) \\ = {} & \alpha KI^*US*(x_1z_2 - 1) - \phi KI^*ES^*(y_1z_2 - 1) \\ & - (\delta+\lambda)ES^*(y_1 - 1) \end{aligned} \tag{26}$$

$$\begin{aligned} \frac{dEI(t)}{dt} = {} & \beta(KI(t)US(t) - KI^*US*) \\ & + \phi(KI(t)ES(t) - KI^*ES^*) \\ & - (\delta+\gamma)(EI(t) - EI^*) \\ = {} & \beta KI^*US*(x_1z_2 - 1) + \phi KI^*ES^*(y_1z_2 - 1) \\ & - (\delta+\gamma)EI^*(y_2 - 1) \end{aligned} \tag{27}$$

$$\begin{aligned} \frac{dER(t)}{dt} = {} & -\varepsilon ER(t) + \gamma EI(t) \\ = {} & -\varepsilon ER^*(y_3 - 1) + \gamma EI^*(y_2 - 1) \end{aligned} \tag{28}$$

$$\begin{aligned} \frac{dKS(t)}{dt} = {} & \omega(KI(t)US(t) - KI^*US*) \\ & + \delta(ES(t) - ES^*) \\ & - \phi(KI(t)KS(t) - KI^*KS^*) \\ & - \lambda(KS(t) - KS^*) \\ = {} & \omega KI^*US*(x_1z_2 - 1) + \delta ES^*(y_1 - 1) \\ & - \phi KI^*KS^*(z_1z_2 - 1) - \lambda KS^*(z_1 - 1) \end{aligned} \tag{29}$$

$$\begin{aligned} \frac{dKI(t)}{dt} = {} & \beta(KI(t)US(t) - KI^*US*) \\ & + \phi(KI(t)KS(t) - KI^*KS^*) \\ & + \delta(EI(t) - EI^*) \\ & - \gamma(KI(t) - KI^*) \\ = {} & \beta KI^*US*(x_1z_2 - 1) + \phi KI^*KS^*(z_1z_2 - 1) \\ & + \delta EI^*(y_2 - 1) - \gamma KI^*(z_2 - 1) \end{aligned} \tag{30}$$

$$\begin{aligned} \frac{dKR(t)}{dt} = {} & -\varepsilon(KR(t) - KR^*) + \gamma(KI(t) - KI^*) \\ = {} & -\varepsilon KR^*(z_3 - 1) + \gamma KI^*(z_2 - 1) \end{aligned} \tag{31}$$

Substituting (25)–(31) into (24), we get the following:

$$\begin{aligned} \frac{dL(t)}{dt} = {} & [A(\alpha+\omega+2\beta)KI^*US^* + |!\phi KI^*KS^* + \phi KI^*ES^* \\ & - B\gamma KI^* + C\gamma KI^*]g(z_2) \\ & + (A-1)\varepsilon ER^*g(y_3) - A\varepsilon ER^*g\left(\frac{y_3}{x_1}\right) \\ & + A[\varepsilon ER^* + \varepsilon KR^* + \lambda ES^* + \lambda KS^* \\ & - (\alpha+\omega+2\beta)KI^*US^*]g\left(\frac{1}{x_1}\right) \end{aligned}$$

$$
\begin{aligned}
&+ (A-C)\,\varepsilon KR^{*} g\left(z_3\right) - A\varepsilon KR^{*} g\left(\frac{z_3}{x_1}\right) \\
&+ \left[A\left(\alpha+\omega+2\beta\right)\right. \\
&\left.- \left(\alpha+\omega+\beta+B\beta\right)\right] KI^{*}US^{*} g\left(x_1 z_2\right) \\
&+ \left(A\lambda KS^{*} - \lambda KS^{*} - B\phi KI^{*}KS^{*}\right) g\left(z_1\right) \\
&- A\lambda KS^{*} g\left(\frac{z_1}{x_1}\right) \\
&+ \left[\alpha KI^{*}US^{*} - \phi KI^{*}ES^{*} - \left(\delta+\lambda\right) ES^{*}\right] g\left(\frac{1}{y_1}\right) \\
&- \alpha KI^{*}US^{*} g\left(\frac{x_1 z_2}{y_1}\right) + \left(A-1\right)\lambda ES^{*} g\left(y_1\right) \\
&- A\lambda ES^{*} g\left(\frac{y_1}{x_1}\right) \\
&+ \left[\beta KI^{*}US^{*} + \phi KI^{*}ES^{*} - \left(\delta+\gamma\right) EI^{*}\right] g\left(\frac{1}{y_2}\right) \\
&- \beta KI^{*}US^{*} g\left(\frac{x_1 z_2}{y_2}\right) - \phi KI^{*}ES^{*} g\left(\frac{y_1 z_2}{y_2}\right) \\
&+ \left(B-1\right) EI^{*} g\left(y_2\right) \\
&- \left(\varepsilon ER^{*} - \gamma EI^{*}\right) g\left(\frac{1}{y_3}\right) - \gamma EI^{*} g\left(\frac{y_2}{y_3}\right) \\
&+ \left(\omega KI^{*}US^{*} + \delta ES^{*} - \phi KI^{*}KS^{*} - \lambda KS^{*}\right) g\left(\frac{1}{z_1}\right) \\
&- \omega KI^{*}US^{*} g\left(\frac{x_1 z_2}{z_1}\right) \\
&- \delta ES^{*} g\left(\frac{y_1}{z_1}\right) + \left(B-1\right)\phi KI^{*}KS^{*} g\left(z_1 z_2\right) \\
&- \beta KI^{*}US^{*} g\left(x_1\right) \\
&+ B\left(\beta KI^{*}US^{*} + \phi KI^{*}KS^{*} + \delta EI^{*} - \gamma KI^{*}\right) g\left(\frac{1}{z_2}\right) \\
&- B\delta EI^{*} g\left(\frac{y_2}{z_2}\right) - C\left(\varepsilon KR^{*} - \gamma KI^{*}\right) g\left(\frac{1}{z_3}\right) \\
&- C\gamma KI^{*} g\left(\frac{z_2}{z_3}\right) \qquad (32)
\end{aligned}
$$

Next, we let $A(\alpha+\omega+2\beta)KI^{*}US^{*} + \phi KI^{*}KS^{*} + \phi KI^{*}ES^{*} - B\gamma KI^{*} + C\gamma KI^{*} = 0$, i.e., $B = \frac{A(\alpha+\omega+2\beta)US^{*}+\phi KS^{*}+\phi ES^{*}+C\gamma}{\gamma} > 0$. By choosing appropriate values of A, $B$and C, i.e., $0 < B < 1$ and $0 < A < C < 1$, which indicates that $A-1<0$, $A-C<0$, and $B-1<0$, $A\lambda KS^{*} - \lambda KS^{*} - B\phi KI^{*}KS^{*} < 0$ and $A(\alpha+\omega+2\beta) - (\alpha+\omega+\beta+B\beta) < 0$.

Simultaneously, combining this with (22) results in $dL(t)/dt \le 0$, and $dL(t)/dt = 0$ if and only if at the information equilibrium point $E^{*} = (US^{*}, ES^{*}, EI^{*}, ER^{*}, KS^{*}, KI^{*}, KR^{*})$.

Therefore, according to the LaSalle's invariance principle, the information equilibrium point of the CCDIDM is globally asymptotically stable for $R_0 > 1$.

REFERENCES

[1] L. Atzori, A. Iera, and G. Morabito, "SIoT: Giving a social structure to the Internet of Things," *IEEE Commun. Lett.*, vol. 15, no. 11, pp. 1193–1195, Nov. 2011.

[2] M. M. Rad et al., "Social Internet of Things: Vision, challenges, and trends," *Hum.-Centric Comput. Inf. Sci.*, vol. 10, no. 1, pp. 1–40, 2020.

[3] S. Rho and C. Yu, "Social Internet of Things: Applications, architectures and protocols," *Future Gener. Comput. Syst.*, vol. 82, no. 5, pp. 667–668, 2018.

[4] P. He and T. Tang, "Community - oriented Multimedia content maximization mechanism in social Internet of Things," *IEEE Access*, vol. 8, pp. 22826–22833, 2020.

[5] M. Venus, M. R. Ami, and D. Aso, "Trust-based friend selection algorithm for navigability in social Internet of Things," *Knowl.-Based Syst.*, vol. 232, no. 1, 2021, Art. no. 107479.

[6] Y. Yi, Z. Zhang, L. T Yang, X. Deng, L. Yi, and X. Wang, "Social interaction and information diffusion in social Internet of Things: Dynamics, cloud-edge, traceability," *IEEE Internet Things J.*, vol. 8, no. 4, pp. 2177–2192, Feb. 2021.

[7] C. Jiang et al., "An operator-based approach for modeling influence diffusion in complex social networks," *J. Social Comput.*, vol. 2, no. 2, pp. 166–182, Jun. 2021.

[8] B. Wu et al., "Public opinion dissemination with incomplete information on social network: A study based on the infectious diseases model and game theory," *Complex Syst. Model. Simul.*, vol. 1, no. 2, pp. 109–121, Jun. 2021.

[9] M. Muhlmeyer, S. Agarwal, and J. Huang, "Modeling social contagion and information diffusion in complex socio-technical systems," *IEEE Syst. J.*, vol. 14, no. 4, pp. 5187–5198, Dec. 2020.

[10] L. Atzori, A. Iera, and G. Morabito, "The Internet of Things: A survey," *Comput. Netw.*, vol. 54, no. 15, pp. 2787–2805, 2010.

[11] J. Gubbi et al., "Internet of things (IoT): A vision, architectural elements, and future directions," *Future Gener. Comput. Syst.*, vol. 29, no. 7, pp. 1645–1660, 2013.

[12] A. Seyfollahi and A. Ghaffari, "Reliable data dissemination for the Internet of Things using Harris hawks optimization," *Peer-to-Peer Netw. Appl.*, vol. 13, no. 6, pp. 1886–1902, 2020.

[13] J. Wang, C. Jiang, Z. Han, and L. Hanzo, "Internet of vehicles: Sensing-aided transportation information collection and diffusion," *IEEE Trans. Veh. Technol.*, vol. 67, no. 5, pp. 3813–3825, May 2018.

[14] C. A. Kerrache et al., "TACASHI: Trust-aware communication architecture for social internet of vehicles," *IEEE Internet Things J.*, vol. 6, no. 4, pp. 5870–5877, Aug. 2019.

[15] J. Sun, H. Xiong, S. Zhang, X. Liu, J. Yuan, and R. H. Deng, "A secure flexible and tampering-resistant data sharing system for vehicular social networks," *IEEE Trans. Veh. Technol.*, vol. 69, no. 11, pp. 12938–12950, Nov. 2020.

[16] D. O. Kang, J. H. Choi, J. Y. Jung, K. Kang, and C. Bae, "SDIF: Social device interaction framework for encounter and play in smart home service," *IEEE Trans. Consum. Electron.*, vol. 62, no. 1, pp. 85–93, Feb. 2016.

[17] K. C. Chung and S. W. J. Liang, "An empirical study of social network activities via social Internet of Things (SIoT)," *IEEE Access*, vol. 8, pp. 48652–48659, 2020.

[18] J. Eom et al., "Using social Internet of Things (SIoT) demand side management on the Plant," in *Proc. IEEE 8th Int. Conf. Ubiquitous Future Netw.*, 2016, pp. 685–687.

[19] C. Marche, M. Nitti, and V. Pilloni, "Energy efficiency in smart building: A comfort aware approach based on social Internet of Things," in *Proc. IEEE Glob. Internet Things Summit*, 2017, pp. 1–6.

[20] M. Newman, "The spread of epidemic disease on networks," *Phys. Rev. E Stat. Nonlinear Soft Matter Phys.*, vol. 66, no. 1, 2002, Art. no. 016128.

[21] Z. Liu, Y. C. Lai, and N. Ye, "Propagation and immunization of infection on general networks with both homogeneous and heterogeneous components," *Phys. Rev. E Stat. Nonlinear Soft Matter Phys.*, vol. 67, no. 3, 2003, Art. no. 031911.

[22] X. Wu, Y. Xiao, X. Liang, and Q. Li, "A dynamic information dissemination model based on implicit link and social influence," *IEEE Trans. Comput. Social Syst.*, vol. 8, no. 2, pp. 345–354, Apr. 2021.

[23] M. Ran and J. Chen, "An information dissemination model based on positive and negative interference in social networks," *Phys. A: Stat. Mech. Appl.*, vol. 572, no. 1, 2021, Art. no. 125915.
[24] L. Feng et al., "Modeling and stability analysis of worm propagation in wireless sensor network," *Math. Problems Eng.*, vol. 2015, no. 1, pp. 1–8, 2015.
[25] Z. Ning, X. Wang, X. Kong, and W. Hou, "A social-aware group formation framework for information diffusion in narrowband Internet of Things," *IEEE Internet Things J.*, vol. 5, no. 3, pp. 1527–1538, Jun. 2018.
[26] O. Yagan, D. Qian, J. Zhang, and D. Cochran, "Conjoining speeds up information diffusion in overlaying social-physical networks," *IEEE J. Sel. Areas Commun.*, vol. 31, no. 6, pp. 1038–1048, Jun. 2013.
[27] S. Qian et al., "Many-to-many matching for social-aware minimized redundancy caching in D2D-enabled cellular networks – sciencedirect," *Comput. Netw.*, vol. 175, no. 1, 2020, Art. no. 107249.
[28] L. Yao et al., "Things of interest recommendation by leveraging heterogeneous relations in the Internet of Things," *ACM Trans. Internet Technol.*, vol. 16, no. 2, pp. 1–25, 2016.
[29] Y. Ma, W. Liang, J. Li, X. Jia, and S. Guo, "Mobility-Aware and delay-sensitive service provisioning in mobile edge-cloud networks," *IEEE Trans. Mobile Comput.*, vol. 21, no. 1, pp. 196–210, Jan. 2022.
[30] X. Wang, Y. Han, V. C. M. Leung, D. Niyato, X. Yan, and X. Chen, "Convergence of edge computing and deep learning: A comprehensive survey," *IEEE Commun. Surv. Tut.*, vol. 22, no. 2, pp. 869–904, Apr.–Jun. 2020.
[31] P. Dreessche and J. Watmough, "Reproduction numbers and sub-threshold endemic equilibria for compartmental models of disease transmission," *Math. Biosci.*, vol. 180, no. 12, pp. 29–48, 2002.
[32] J. Li et al., "Dynamical analysis of rumor spreading model in multi-lingual environment and heterogeneous complex networks," *Inf. Sci.*, vol. 536, no. 1, pp. 391–408, 2020.
[33] Z. Cao et al., "Nontrivial periodic solution of a stochastic seasonal rabies epidemic model," *Physica A: Stat. Mech. Appl.*, vol. 545, no. 1, 2020, Art. no. 123361.
[34] Z. Zhang et al., "Dynamics of information diffusion and its applications on complex networks," *Phys. Rep.*, vol. 651, pp. 1–34, 2016.
[35] W. Wang et al., "Coevolution spreading in complex networks," *Phys. Rep.*, vol. 820, pp. 1–51, 2019.
[36] Z. Wang et al., "Coupled disease–behavior dynamics on complex networks: A review," *Phys. Life Rev.*, vol. 15, pp. 1–29, 2015.

Yuexia Zhang (Member, IEEE) (1978-) born in Henan, China, she received the M.S. and Ph.D. degrees in information and communication engineering from the Beijing University of Posts and Telecommunications, Beijing, China, in 2008. Since 2019, she has been a Full Professor with the School of Information and Communication Engineering, Beijing Information Science and Technology University. Her research interests include wireless cooperative communication technology, ultra-wideband technology, and wireless positioning technology.

Lie Zou (1997-) born in Ningxia, China, he received the bachelor's degree from the School of Information and Communication Engineering, Xi'an University of Posts and Telecommunications, Xi'an, China, in 2019. He is currently working toward the master's degree with the School of Information and Communication Engineering, Beijing Information Science and Technology University, Beijing, China. His research focuses on complex network public opinion communication analysis.

Dawei Pan (1998-) born in Beijing, China, he received the bachelor's degree in information and communication engineering in 2020 from Beijing Information Science and Technology University, Beijing, China, where he is currently working toward the master's degree. His research focuses on complex network public opinion communication analysis.